Simulating device size effects on magnetization pinning mechanisms in spin valves[a)]

J. O. Oti, R. W. Cross, and S. E. Russek
National Institute of Standards and Technology, Boulder, Colorado 80303

Y. K. Kim
Quantum Peripherals Colorado, Inc., Louisville, Colorado 80028

The effects of magnetostatic interactions on the giant magnetoresistive (GMR) response of NiFe/Cu/NiFe spin valves are studied using an analytical model. The model is applicable to devices small enough for the magnetic layers to exhibit single-domain behavior. Devices having lengths in the track-width direction of 10 μm and interlayer separations of 4.5 nm are studied. Stripe heights are varied from 0.5 to 2 μm. The magnetization of one magnetic layer is pinned by a transverse pinning field that is varied from 0 to 24 kA/m (300 Oe). GMR curves for transverse fields are calculated. At zero external field the magnetization of the layers shows a tendency to align themselves antiparallel in the transverse direction. This results in an offset from the ideal biasing of the device. Broadening of the curves due to shape anisotropy occurs with decreasing stripe height and increasing magnetic layer thickness, and the magnetization in the pinned layer becomes less stable. © *1996 American Institute of Physics.* [S0021-8979(96)56408-X]

INTRODUCTION

Spin valves[1] are being actively investigated as promising read-head materials in ultrahigh-denisty magnetic recording. This is because of their relatively simple structure and high sensitivity to external fields. In this work, spin valves are studied using an analytical model that is an extension to two layers of a Stoner–Wohlfarth single-layer model.[2,3] Our model differs from other analytical spin-valve models,[4] by including interlayer magnetostatic interaction effects and the ability to model magnetic layers using general ellipsoidal shapes.

The micromagnetic model is applicable to devices that are small enough in size for the magnetic layers to exhibit single-domain behavior. The transition width of a Néel domain wall in a magnetic thin film increases with decreasing film thickness. For a small enough sample, the transition width exceeds the film dimensions, so that the film is no longer capable of sustaining domain walls. The film then becomes single domain. In Ref. 2, single-domain behavior was observed in magnetoresistive NiFe films having stripe heights less than 2 μm and film thicknesses less than 10 nm.

Figure 1 shows schematically the three-layer spin-valve structure studied in this work. Two NiFe layers of length l, stripe height w, and thickness t are separated by a Cu spacer layer of thickness d. Current I flows longitudinally through the device. The magnetization **M** of the top NiFe layer is exchange pinned transversely by an antiferromagnetic overcoat layer (not shown in the figure), while the magnetization of the bottom layer is free to rotate. The device is ideally biased if, in the absence of an external field, the magnetization of the layers orient perpendicular to each other in the plane of the film, as shown in Fig. 1(a). Figure 1(b) shows the giant magnetoresistance (GMR) response curve of an ideally biased spin valve. A description of the micromagnetic model is given in the following section. The model is used in a systematic study of the dependence of GMR response on stripe height and pinning-field strength.

MODEL OF SPIN VALVE

The magnetic layers of a spin valve are treated as single-domain films, and their magnetic behaviors are modeled using the Stoner–Wohlfarth coherent rotation model of the magnetization reversal of a uniformly magnetized ellipsoid. Brown[5] showed that the magnetic behavior of any uniformly

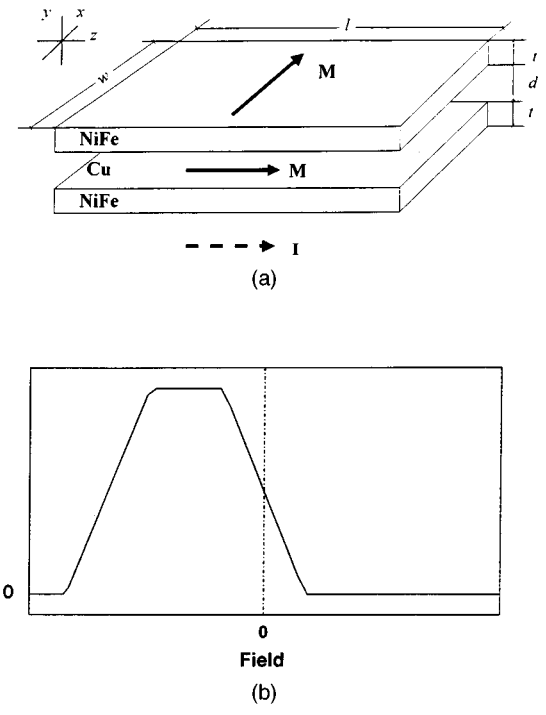

FIG. 1. (a) Schematic of modeled spin valve structure; (b) GMR response of ideally biased spin valve.

[a)]Contribution of the National Institute of Standards and Technology, not subject to copyright.

 0021-8979/96/79(8)/6386/3/$10.00

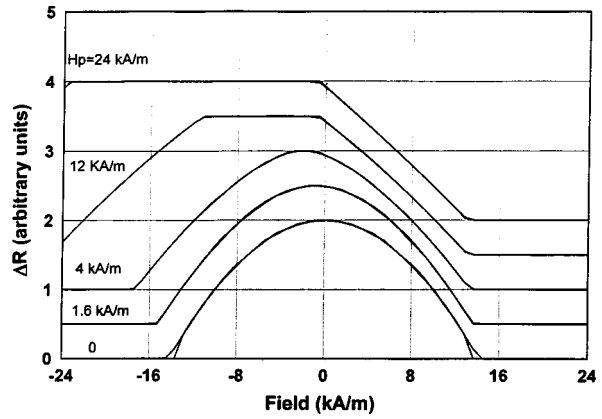

(a)

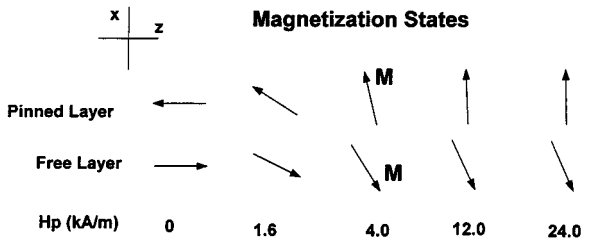

(b)

FIG. 2. (a) GMR response curves as a function pinning field H_p, for devices with stripe height $w=2$ μm and magnetic layer thickness $t=10$ nm. The curves are displaced vertically from each other for clarity; (b) magnetization states at zero field of the devices in the pinned layer (top arrows) and free layer (bottom arrows).

magnetized body could be modeled as that of an appropriate equivalent ellipsoid, which has the same principal axes and volume as the actual body. For a body in the form of a rectangular film the demagnetizing factors of the equivalent ellipsoid along the principal axes are equal to the magnitudes of the volume-average demagnetizing fields per unit magnetization inside the film, when it is magnetized along its principal axes. The field sources of a uniformly magnetized film are the surface magnetic charges formed on its bounding faces. The field due to such a face can be expressed in closed form.[6]

The free energy density of the pinned magnetic layer, consisting of the self-demagnetization and the applied field terms, is given by the expression

$$W=\tfrac{1}{2}M_s^2(N_x\alpha^2+N_y\beta^2+N_z\gamma^2) - |\mathbf{H_o}+\mathbf{H_p}+\mathbf{H_m}(M_s')|M_s(l\alpha+m\beta+n\gamma), \qquad (1)$$

where $\mathbf{H}_o$ is the externally applied field; $\mathbf{H}_p$ is the pinning field; $\mathbf{H}_m(M_s')$ is the interlayer magnetostatic interaction field, and is equal to the volume-average field acting on the film due to the magnetization M_s' of the free layer; α, β, and γ are the direction cosines of the magnetization of the film M_s; l, m, and n are the direction cosines of the total field $\mathbf{H}_o+\mathbf{H}_p+\mathbf{H}_m(Ms_s')$, and N_x, N_y, and $N_z(N_x+N_y+N_z=1)$ are the demagnetizing factors along the three principal axes of the film.

Surface charges on the boundaries of the actual rectangular geometry of the magnetic film are the field sources used in calculating $\mathbf{H}_m$. Other fields, such as the self-field due to current flowing through the device, and possible effective exchange interaction field between the magnetic layers, may be included in the applied-field term in Eq. (1) if needed. These additional field terms were not considered in this work. An expression similar to Eq. (1) follows for the energy density of the free layer, by interchanging the roles of M_s and M_s' and omitting the pinning field term. For the free layer, $\mathbf{H}_m$ is the interlayer magnetostatic interaction field acting on it due to the magnetization of the pinned layer.

The direction cosines α, β, and γ are related to the azimuthal and polar angular coordinates θ_M, ϕ_M of the magnetization vector, by $\alpha=\sin\theta_M\cos\phi_M$, $\beta=\sin\theta_M\sin\phi_M$, and $\gamma=\cos\theta_M$. The spin valve is subjected to a uniform external field that is varied step-wise. The magnetization dependence of $\mathbf{H}_m$ necessitates the use of iterative methods in minimizing the energy of the interacting magnetic layers. The expression in parenthesis in the self-demagnetization term of Eq. (1) is precomputed and stored as a function of the angular coordinates. These values are calculated only for one quadrant of space; the values for other quadrants can be found by symmetry. Beginning from an initial magnetization state of the layers, the stored values are used to compute the energy functional $W(\theta_M,\phi_M)$ according to Eq. (1) in each of the magnetic layers. The angular coordinates corresponding to the minima of $W(\theta_M,\phi_M)$ in the magnetic layers are found and used to obtain the first approximations of the magnetization of the layers. These approximations are used to recalculate $\mathbf{H}_m$ and a new energy functional, from which the next approximation to the magnetization is obtained. This procedure is repeated until the magnetization of the layers converges to equilibrium. During iteration, the $(l\alpha+m\beta+n\gamma)$ term continually changes as $\mathbf{H}_m$ changes with the magnetization of the layers. The initial magnetization states used at the beginning of the iteration are the solution states from the preceding external field. The first solution when the external field is initially applied is obtained by assuming that the magnetization of the layers are initially pointing in the positive z direction. The solution space for the magnetization of a single layer depends on the history of the magnetization process, and the search for possible solutions having angular coordinate $\theta_M=0$ requires special treatment. The switching of the magnetization of each layer occurs as its free energy reaches an unstable threshold, changing from a minimum to maximum energy state. These issues are described in detail in Ref. 3. The change in the magnetoresistance of the spin valve is calculated using the expression $\Delta R=1-\cos\theta$, where θ is the angle between the magnetization vectors of the layers.

SIMULATION RESULTS

The spin valves simulated in this work have length $l=10$ μm, nonmagnetic spacer thickness $d=4.5$ nm, and magnetic layers with magnetization $M=800$ kA/m. The GMR response curves for the devices are calculated for an external transverse field (acting along x axis in Fig. 1) that is cycled between ± 24 kA/m (300 Oe). GMR response curves calculated

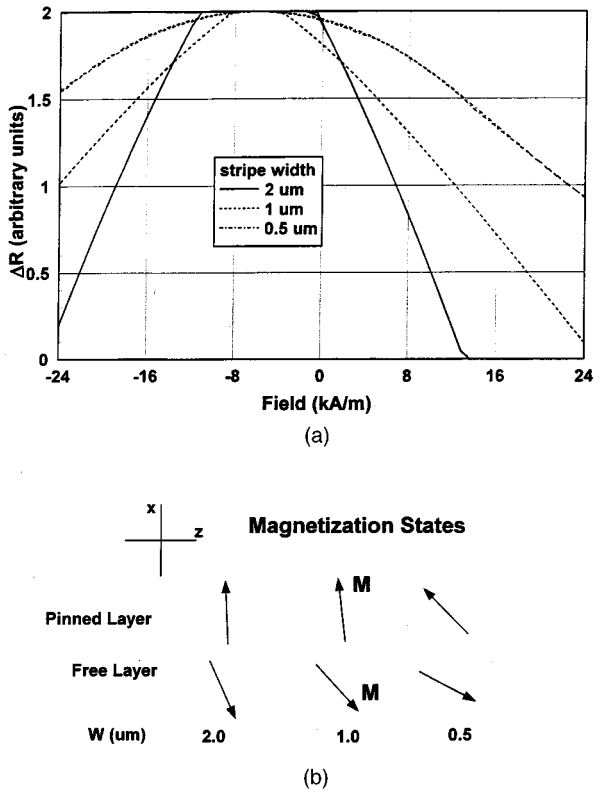

FIG. 3. (a) GMR response curves as a function of stripe width w, for devices with magnetic layer thickness $t=10$ nm and pinning field $H_p=12$ kA/m; (b) magnetization states at zero field of the devices in the pinning (top arrows) and free (bottom arrows) layers.

using different pinning fields, for devices having stripe height $w=2$ μm and magnetic layer thickness $t=10$ nm, are plotted in Fig. 2(a). The zero-field magnetization states of the devices given by the orientations of the magnetization vectors in the pinned and free layers are shown in Fig. 2(b). The shape anisotropy of the magnetic layers causes the magnetization vectors to lie completely in the plane of the magnetic films. For moderately pinned devices ($H_p \leqslant 4$ kA/m), self-demagnetizing fields in the pinned layer result in considerable canting, away from the transverse direction, of the magnetization vectors at zero field. Pinning is improved as H_p is increased.

Magnetostatic coupling between the magnetic layers favors the antiparallel orientation of the magnetization of the layers. This antiparallel orientation is pronounced in moderately pinned devices. In strongly pinned devices ($H_p=12$ and 24 kA/m), the rotation of the free layer is opposed by the self-demagnetization of the layer. Interlayer magnetostatic interaction thus results in the deviation of the GMR responses of the spin valves from that of the ideal biased state of Fig. 1. The positive saturation fields of the GMR curves decrease slightly as the pinning field is increased. This is due to a reduction in the work required to rotate the magnetization of both magnetic layers toward parallel alignment in the transverse direction against the interlayer magnetostatic interactions opposing this rotation. The peaks of the GMR curves get broader and flatter as the pinning field is increased, and the negative saturation fields increase.

Self-demagnetization effects in the devices increase as stripe heights are made smaller. The effect of decreasing the stripe height on the GMR response and magnetization states of the devices is shown in Fig. 3. The figure was obtained for devices with magnetic layer thickness of 10 nm and pinning field 12 kA/m. Decreasing the stripe height increases the canting of the magnetization of the pinned layers and increases the broadening of the GMR curves.

DISCUSSION

An analytical micromagnetic model of interacting single-domain films was used in this work to study the dependence on device sizes and pinning field strengths of the GMR responses of spin valves having identical magnetic layers. The calculation of self-demagnetizing and magnetostatic fields can be modified to take into account nonuniform magnetization in the magnetic layers.[7] The simulations show offsets in the ideal biasing of devices due to interlayer magnetostatic interaction. The GMR curves broaden as the self-demagnetization in the magnetic layers increases as the stripe height is decreased. Thus, for moderately pinned devices, self-demagnetization results in the canting of the magnetization of the pinned layers. The behavior of the devices is sensitive to their linear dimensions; the offset in biasing can be corrected by the judicious choice of device dimensions. For example, if the free layer is made thicker than the pinned layer, the self-demagnetization will oppose the antiparallel rotation of the magnetization, resulting in better biasing.

The model can be extended in a straightforward manner to simulate devices with three or more magnetic layers, and to include interlayer ferromagnetic, antiferromagnetic, and biquadratic exchange interactions between adjacent magnetic layers. More exotic devices can thus be simulated and studied both by selectively applying these interactions among the magnetic layers and by making use of magnetic layers with different magnetic properties and linear dimensions. Self-fields due to current flow in the device can be modeled by adding an appropriate field to the applied field free energy density term of Eq. (1).

[1] B. Dieny, V. Speriosu, S. S. P. Parkin, B. A. Gurney, D. R. Wilhoit, and D. Mauri, Phys. Rev. B **43**, 1297 (1991).
[2] R. W. Cross, J. O. Oti, S. E. Russek, T. Silva, and Y. K. Kim, IEEE Trans. Magn. **31**, 3358 (1995).
[3] C. E. Johnson. J. Appl. Phys. **33**, 2515 (1962).
[4] M. R. Parker, H. Fujiwara, S. Hossain, and W. E. Webb, IEEE Trans. Magn. **MAG-31**, 2618 (1995).
[5] W. F. Brown, *Magnetostatic Principles in Ferromagnetism* (North-Holland, Amsterdam, 1962), pp. 49–53.
[6] J. O. Oti, IEEE Trans. Magn. **MAG-29**, 1265 (1993).
[7] H. N. Bertram, *Theory of Magnetic Recording* (Cambridge University Press, Cambridge, 1994), pp. 170–176.